[Article ID] 1003- 6326(2001)02- 0254- 04

Nanocrystallization of $Al_{80}Ni_6Y_8Co_4Cu_2$ amorphous alloy①

BIAN Zan(边 赞)[1], SUN Yu-feng(孙玉峰)[2], HE Guo(何 国)[1], CHEN Guo-liang(陈国良)[1]
(1. State Key Laboratory for Advanced Metals and Materials, University of Science and Technology Beijing;
2. School of Materials Science and Technology, University of Science and Technology Beijing,
Beijing 100083, P. R. China)

[Abstract] Nanoscale α(Al) phase with a size of 15 nm was precipitated from $Al_{80}Ni_6Y_8Co_4Cu_2$ amorphous ribbons after annealing. The microhardness increases with increasing the crystallization volume fraction of nanoscale α(Al) phase. The combination effect of alloy strengthening and dispersion strengthening is main reason for the increase of microhardness. The formation of intermetallic compound (Al_3Ni) with a small volume fraction leads to the decrease of microhardness resulting from the depletion of the solute elements in the residual amorphous matrix and the weakening of alloy strengthening. With increasing the volume fraction of intermetallic compound, microhardness increases again due to dispersion strengthening of nanoscale intermetallic compound.

[Key words] nanoscale α(Al) particle; alloy strengthening; dispersion strengthening; microhardness
[CLC number] TG139.8; TG111.5 [Document code] A

1 INTRODUCTION

Nanocrystalline Al-rich glass alloys have attracted great attention as a new material due to its much higher specific strength than the highest strength of conventional crystalline Al-based alloys[1]. Refs. [2, 3] reported that the fracture strength is above 1 000 GPa for Al-rich amorphous alloys by dispersion of nanoscale α(Al) particles. So, it is very important to develop new Al-based alloy systems with large glass formation ability or strong tendency to form nanocrystalline materials[4, 5]. In this paper, $Al_{80}Ni_6Y_8Co_4Cu_2$ alloy is designed and its amorphous ribbons is prepared, the aims are to investigate the precipitation process and the growth mechanism of α(Al) particles and to discuss dependence of mechanical properties on the crystallization volume fraction of nanoscale α(Al) particles.

2 EXPERIMENTAL

Al-based alloys with a nominal composition of $Al_{80}Ni_6Y_8Co_4Cu_2$ (mole fraction, %) were prepared by arc melting a mixture of appropriate amounts of pure metals including Al(99.999%), Ni(99.99%), Y(99.99%), Co(99.99%) and Cu(99.99%) under pure argon atmosphere together. The master ingots were surface-polished, broken into small pieces and put into quartz tubes and then melted by induction under argon atmosphere. The melt was used to produce amorphous ribbons with a width of 3.0 mm and thickness of 20~ 30 μm by the single-roller melt spinning technique (the diameter of copper roller is 200 mm). The amorphous ribbons were annealed isothermally under pure argon atmosphere. X-ray diffraction (CuK_α) was used to identify precipitated phases. Thermal stability associated with glass transition and suppercooled liquid region was examined by differential scanning calorimeter (DSC). The microstructure of samples was observed by transmition electron microscope (TEM). TEM samples were thinned electrolytically by jet polishing at 250 K in a solution of 33% (volume fraction) nitric acid and 67% (volume fraction) methanol, And the microhardness of $Al_{80}Ni_6Y_8Co_4Cu_2$ alloy annealed at different states was measured by using Nanoindenter.

3 RESULTS AND ANALYSES

Fig. 1 shows X-ray diffraction patterns of $Al_{80}Ni_6Y_8Co_4Cu_2$ alloy annealed at different states. It can be noticed that nanoscale α(Al) precipitates from the amorphous matrix after isothermal annealing for 10 min and 20 min at 573 K. DSC curves of $Al_{80}Ni_6Y_8Co_4Cu_2$ alloy at different annealing conditions are shown in Fig. 2. The continuous decrease of first crystallization peak implies that the first peak corresponds to the crystallization of nanoscale α(Al) phase. Fig. 3 shows TEM bright-field image of $Al_{80}Ni_6Y_8Co_4Cu_2$ alloy after annealing for 10 min at 573 K. It can be seen that α(Al) particles with a size of less than 15 nm disperse on the amorphous matrix.

Fig. 4 is the isothermal DSC curve of $Al_{80}Ni_6Y_8Co_4Cu_2$ alloy for the first transformation. It is noticed specially that no incubation stage for the precipitation of α(Al) phase is observed in the curve, which implies that the precipitation of α(Al) phase takes

① [Foundation item] Project (863- 715- 005- 0130) supported by the National Advanced Materials Committee of China and project (2992010) supported by the Natural Science Foundation of Beijing City [Received date] 2000- 03- 13; [Accepted date] 2000- 10- 08

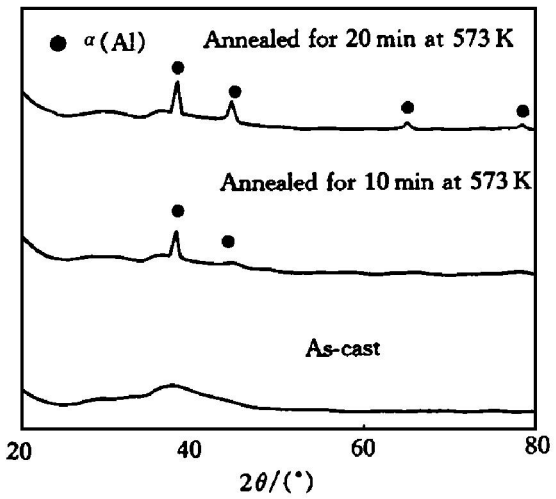

Fig. 1 X-ray diffraction patterns of $Al_{80}Ni_6Y_8Co_4Cu_2$ alloy annealed for different times at 573 K

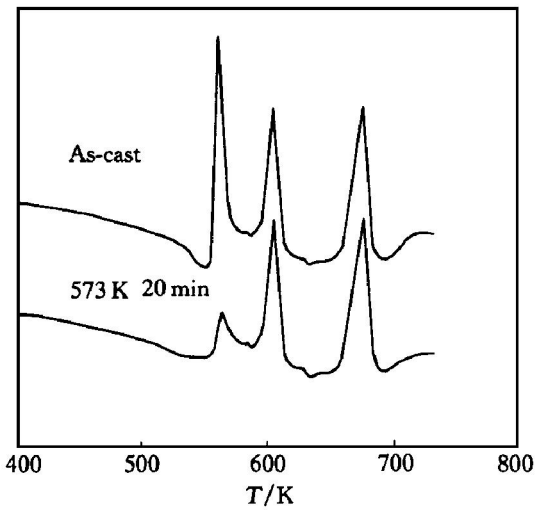

Fig. 2 DSC curves of $Al_{80}Ni_6Y_8Co_4Cu_2$ alloy annealed for different times at 573 K

place by the growth process of pre-existent α(Al) nuclei without nucleation stage in the present alloy. This result is consistent with the data reported by Calin et al[6] in Al-Ni-Y alloy systems, Clavaguere et al[7] in Al-Ni-Nd-Cu alloy systems and Tsai et al[8] in Al-Ni-Ce alloy systems.

Fig. 5 shows the dependence of the crystallization volume fraction of the primary α(Al) phase on the isothermal annealing time. It can be seen that the crystallization volume fraction of the primary α(Al) phase increases rapidly in the initial stage of crystallization. Fig. 6 shows the microhardness of $Al_{80}Ni_6Y_8Co_4Cu_2$ alloy after different annealing treatments. The microhardness increases with increasing the annealing time, it is about 2.55 GPa for as-cast amorphous alloy and increases significantly in the partially crystallized states, i.e., 3.02 GPa at φ_{crys} = 20%, 3.24 GPa at φ_{crys} = 52%, 3.28 GPa at φ_{crys} = 77%, 3.31 GPa at φ_{crys} = 97.6%. It is obviously observed that the value of microhardness increases slowly when the crystallized volume fraction of α(Al) phase is

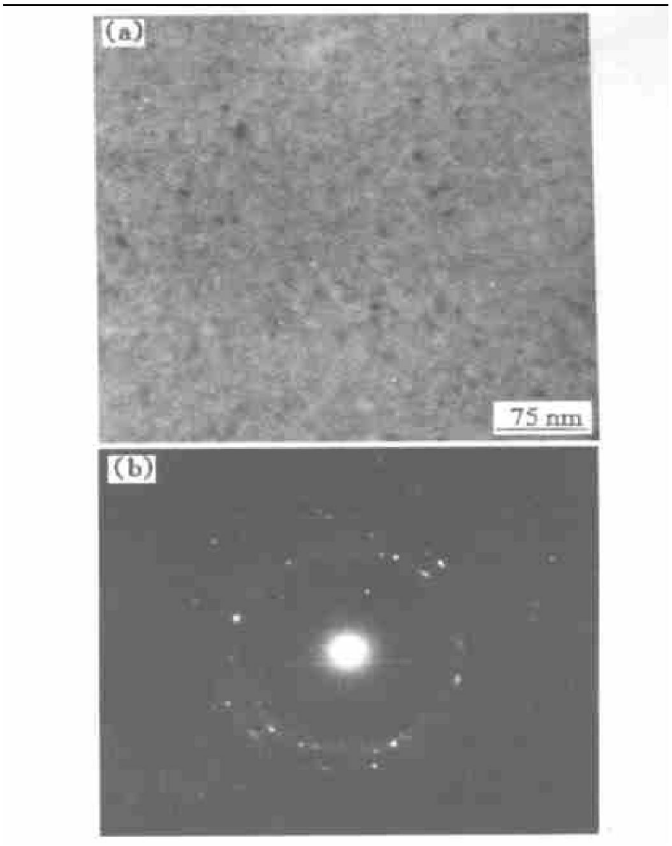

Fig. 3 TEM bright-field image and electron diffraction pattern of $Al_{80}Ni_6Y_8Co_4Cu_2$ alloy after annealed for 20 min at 573 K

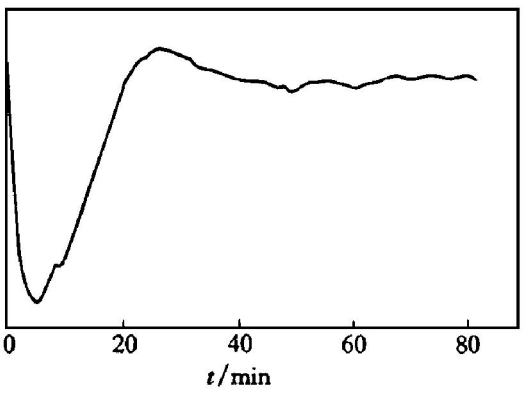

Fig. 4 Isothermal DSC curve of $Al_{80}Ni_6Y_8Co_4Cu_2$ alloy at 573 K

more than 50% and close to a constant value in the end.

Fig. 7 shows X-ray diffraction patterns of $Al_{80}Ni_6Y_8Co_4Cu_2$ alloy annealed for different times at 623 K. After isothermally annealing for 5 min, only α(Al) phase precipitates from the amorphous matrix. However, intermetallic compound begin to precipitate after annealing for 10 min. DSC curves of $Al_{80}Ni_6Y_8Co_4Cu_2$ alloy after different annealing treatments are shown in Fig. 8. In the curves, the intensity of the first peak reduces for samples annealed for 3 min at 623 K (Fig. 8(b)), which means that only α(Al) phase precipitates in this case. It is consistent

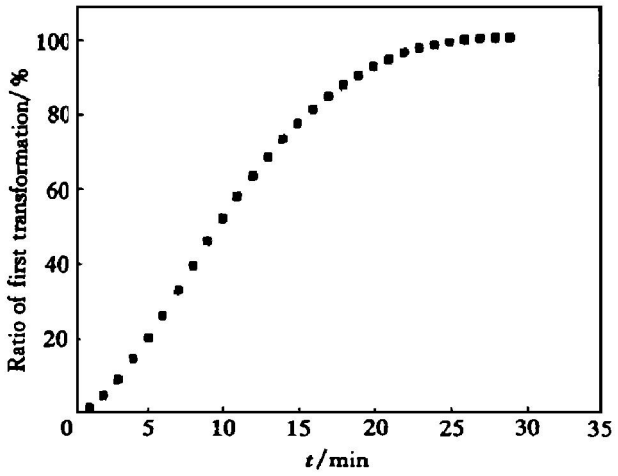

Fig. 5 Dependence of crystallization volume fraction of primary α(Al) phase on isothermal annealing time

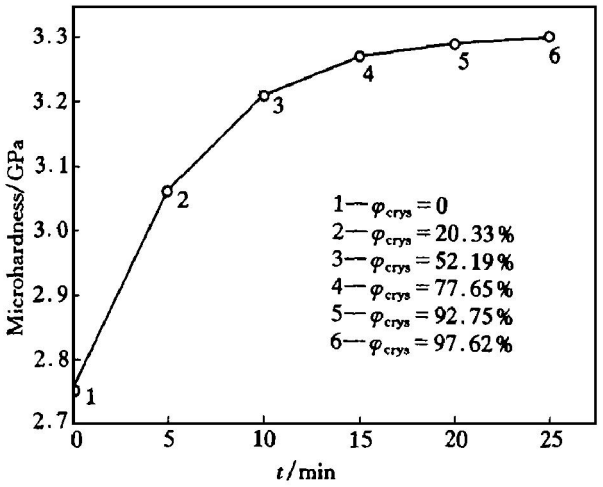

Fig. 6 Microhardness of $Al_{80}Ni_6Y_8Co_4Cu_2$ alloy annealed for different times at 573 K

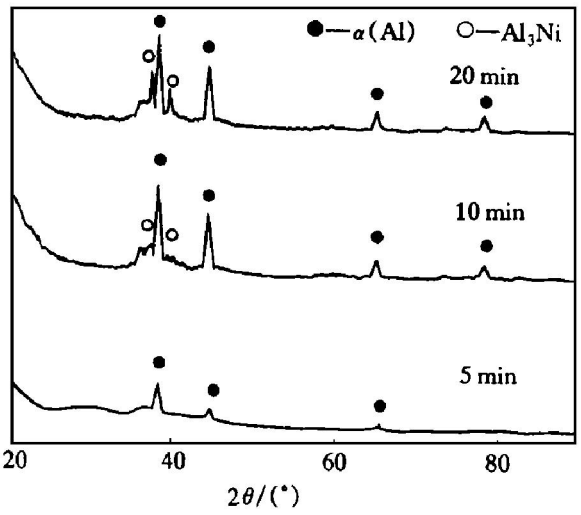

Fig. 7 X-ray diffraction patterns of $Al_{80}Ni_6Y_8Co_4Cu_2$ alloy annealed for different times at 623 K

with the result of X-ray patterns. From Fig. 8(c), it is specially noticed that the first peak disappears and

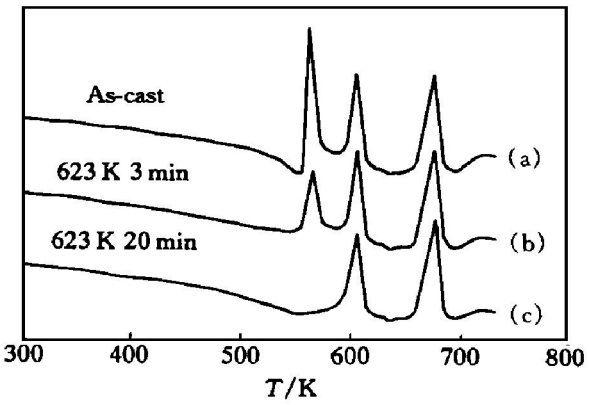

Fig. 8 DSC curves of $Al_{80}Ni_6Y_8Co_4Cu_2$ alloy annealed for different annealing times at 623 K (R = 20 K/min)

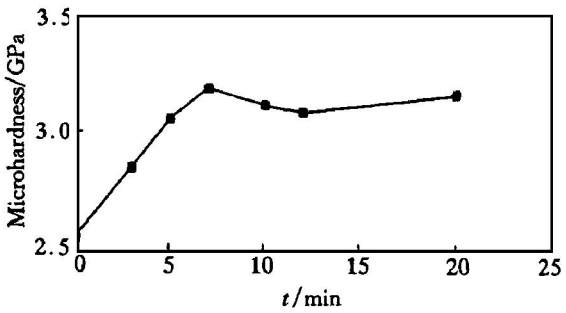

Fig. 9 Microhardness of $Al_{80}Ni_6Y_8Co_4Cu_2$ alloy annealed for different time at 623 K

the second peak also reduces, which means that the first transformation (the precipitation of the primary α(Al) phase) has finished and intermetallic compound Al_3Ni phase begins to precipitate from the residual amorphous matrix. Nanoscale phase with a size of 30 nm disperses to the residual matrix. Fig. 9 is the microhardness of $Al_{80}Ni_6Y_8Co_4Cu_2$ alloy annealed for different times at 623 K. After annealing for short time, the microhardness increases gradually, but after annealing for 10 min, the microhardness decreases slightly, which suggests that the precipitation of intermetallic compound has effect on the microhardness of the alloy. With increasing the annealing time (above 12 min), the microhardness increases again.

4 DISCUSSION

From Fig. 6, the microhardness of $Al_{80}Ni_6Y_8Co_4Cu_2$ amorphous alloy increases with increasing isothermally annealing time at 573 K. Tsai et al[8] reported that the primary α(Al) particles, precipitated by isothermal annealing, have a much lower concentration of the solute element than the residual amorphous matrix in $Al_{87}Ni_{10}Ce_3$ alloy. It implies that the solute elements (Ni, Ce element) are rejected from α(Al) phase and diffuse into the residual amorphous

matrix. In the present alloy, this case also takes place. The solute element (Ni, Co, Cu, Y elements) are also rejected from growing the primary Al phase, which forms the enrichment of the solute elements in the growing front of crystals resulting from their lower diffusivity. So, it is reasonable to infer that the increase of the microhardness is due to the combination role of alloy strengthening and dispersion strengthening resulting from α(Al) particles dispersed on the amorphous matrix. Inoue et al[9] reported that dispersion strengthening of nanoscale α(Al) phase results from its perfect structure and not containing dislocation or other defects. Zhong et al[10, 11] studied the compositional variation of the residual amorphous matrix after the precipitation of α(Al) particles and made a conclusion that the increase of Vicker's hardness in Al-Ni-Y alloy is due to alloy strengthening effect of the residual amorphous matrix.

In order to investigate the effect of alloy strengthening on the mechanical properties, the present amorphous ribbons were annealed for different times at 623 K. The anomalous variation of microhardness can be observed in Fig. 9. As shown in Fig. 9, the precipitation of intermetallic compound leads to the decrease of microhardness at first. After annealing for 3 min and 5 min at 623 K, respectively, only α(Al) particles precipitate and microhardness increases with increasing isothermal time. After annealing for 7 min and 10 min at 623 K, the microhardness starts to decrease gradually. The main reason for it is that the concentration of the solute elements in the residual amorphous matrix decreases due to the precipitation of intermetallic compound. The depletion of the solute elements in the residual amorphous matrix leads to weak bonding among continent element and the softening of the residual amorphous matrix[12, 13]. So, it is not difficult to understand that the microhardness decreases after the formation of intermetallic compound from the residual amorphous matrix. With further increasing annealing time, the dispersion strengthening of nanoscale intermetallic compound compensates for the reduction of microhardness resulting from the depletion of the solute element. So, the microhardness of the alloy increases again.

[REFERENCES]

[1] Horio Y, Inoue A and Masumoto. New Al-based amorphous alloys with high mechanical strength in the Al-Ni-M and Al-Co-M (M= Mn, Fe, Co, Ni) systems [J]. Mater Sci Eng, 1994, A179/A180: 596- 599.

[2] LI Jian-chen, MA Li-jie and YU Yan. Electrodeposition of Al-Mn amorphous alloy [J]. The Chinese Journal of Nonferrous Metals, (in Chinese), 1997, 7(1): 172- 175.

[3] Yeong-Hwan Kim, Inoue A and Masumoto T. Increase in mechanical strength of Al-Ni-Y amorphous alloys by dispersion of nanoscale FCC-Al particles [J]. Mater Trans, JIM, 1991, 32: 331.

[4] Chen H, He Y, Shiflet G J, et al. Mechanical properties of partially crystallized aluminium based metallic glasses [J]. Scripta Metall, 1991, 25: 1421- 1424.

[5] HU Lian-xi, LI Zhi-min, WANG Xiao-lin, et al. Influence of technical parameters on microstructure and properties of nanocrystalline 2024 Al alloy consolidated by hydrostatic extrusion [J]. The Chinese Journal of Nonferrous Metals, (in Chinese), 1999, 9(Suppl. 1): 229- 233.

[6] Calin M and Köster U. Nanocrystallization of Al-Ni-Y and Al-Ni-Nd metallic glasses [J]. Materials Science Forum, 1998, 269- 272; 749- 754.

[7] Clavaguera N, Diego J A, Clavaguera-Mora M T, et al. Nanocrystalline formation of AlNiNdCu materials: a kinetic study [J]. Nanostructured Materials, 1995, 6: 485 - 488.

[8] Tsai A P, Kamiyama T, Kawamura Y, et al. Formation and precipitation mechanism of nanoscale Al particles in Al-Ni base amorphous alloys [J]. Acta Metall, 1997, 45: 1477- 1487.

[9] Inoue A. Fabrication and novel properties of nanostructured Al base alloys [J]. Mater Sci Eng, 1994, A179/A180: 57- 61.

[10] Zhong Z C, Jiang X Y and Greer A L. Nanocrystallization in Al-based amorphous alloys [J]. Philosophical Magazine B, 1997, 76: 505- 510.

[11] Jiang X Y, Zhong Z C and Greer A L. Primary crystallization in an amorphous $Al_{88}Ni_4Y_8$ alloy [J]. Philosophical Magazine B, 1997, 76: 419- 423.

[12] Yeong-Hwan Kim, Inoue A and Masumoto T. Ultrahigh tensile strength of $Al_{88}Ni_9Y_2M_1$ (M= Mn or Fe) amorphous alloys containing finely dispersed FCC-Al particles [J]. Mater Trans, JIM, 1990, 31: 747.

[13] Inoue A. High strength bulk amorphous alloys with low critical cooling rates (overview) [J]. Mater Trans, JIM, 1995, 36: 866- 875.

(Edited by HUANG Jin-song)